J Mater Sci: Mater Electron (2007) 18:575–585
DOI 10.1007/s10854-007-9141-8

Electrodeposition and characterization of CdSe semiconductor thin films

S. M. Rashwan · S. M. Abd El-Wahab · M. M. Mohamed

Received: 23 September 2005 / Accepted: 19 January 2007 / Published online: 30 March 2007

Abstract The electrodeposition of cadmium selenide alloy on glassy carbon and gold electrodes has been studied by electrochemical techniques. Potentiostatic I-t transients were recorded to obtain the nucleation mechanism, while cyclic voltammetry was used to characterize the system. Structural information on the electrodeposited layers was obtained by X-ray diffraction. The experimental results clearly show that the deposition of cadmium selenide alloy on glassy carbon and gold electrodes is a diffusion-controlled process. The nucleation is progressive, and the number of nucleation sites decreases with increasing bath temperature. The deposition of CdSe alloy results in well-defined crystals with hexagonal shape. The films were characterized by optical absorption and electrical resistivity measurements. Films showed a direct band gap of 3.56 eV.

1 Introduction

The thin films of cadmium selenide, which belongs to the $A^{II}B^{VI}$ group of semiconductors, are of great technical interest. The characteristic combination of properties, determined from the band structure, makes cadmium selenide of prime importance in energy conservation problems [1–3]. Usually, the thin films of cadmium selenide are of interest for their application as thin film transistors [4], gas sensors [5, 6], acousto-optical devices [7], vidicones [8], photographic photoreceptors [9], etc.

Cadmium selenide exists in two polymorph modifications: cubic and hexagonal [10]. The structure of cubic modification is of sphalerite type, whereas the hexagonal modification is of wurcite-type structure. The cubic cadmium selenide converts to hexagonal modification at 350–400 °C [11]. Although the number of published papers treating cadmium selenide is rather large [12–18], especially the cubic modification of this semiconductor is one of the least studied $A^{II}B^{VI}$ system. The structure of synthesized cadmium selenide thin films depends on the experimental conditions. Thus, the preparation of thin films of cubic cadmium selenide is a very difficult task. This is in correlation with the relatively small number of published methods [12, 13] for this modification. According to Kainthla and co-workers [14, 15], the prepared cadmium selenide in thin film form, using a method of chemical deposition, is mostly a mixture of cubic and hexagonal modifications. The films deposited from (strongly alkaline) reaction system which is super saturated with $Cd(OH)_2$ have mixed cubic and hexagonal structure, while upon deposition from a clear solution at relatively lower pH value cadmium selenide crystallizes in cubic modification. The sophisticated technologies (such as molecular beam epitaxy, vacuum evaporation, electrodeposition [16–19]) have been mostly used for preparation of cubic CdSe thin films.

The aim of the present work is to study the electrodeposition of CdSe alloys from acidic baths. The effect of bath composition and some operating parameters on cyclic voltammetry and chronoamperometry was investigated. The optical and electrical properties of the obtained thin films are thoroughly investigated.

S. M. Rashwan (✉) · M. M. Mohamed
Chemistry Department, Faculty of Science, Suez Canal University, Ismailia, Egypt
e-mail: DrSalahRashwan@yahoo.com

S. M. Abd El-Wahab
Chemistry Department, Faculty of Science, Ain Shams University, Cairo, Egypt

2 Experimental procedure

The electrolyte solutions were prepared by dissolving SeO_2, $CdSO_4 \cdot 5H_2O$ (Merck-quality) in deionized water. The pH value of the solution was adjusted by using 1 M H_2SO_4. The films were deposited from the solution of various volumetric compositions from 0.1 M $CdSO_4$ + 0.1 M SeO_2.

The cyclic voltammertric and chronoamperometric measurements were carried out in a convention three-electrode cell and were performed using a potentiostat/galvanostat, Model 263A EG&G (Princeton applied research) connected to a computer (X-Y recorder programme, series 2000 Ominographic). A glassy carbon (A = 0.0707 cm^2) or gold (A = 0.0079 cm^2) rods was used as the working electrode, Pt metal as the counter electrode, and saturated calomel electrode (SCE) as the reference electrode, separately. The glassy carbon electrode was polished with γ–Al_2O_3 suspension of 0.1μm particle size. (Gamal, Fisher Scientific, Pittsburgh, PA) for a determinate time, usually 10 s., on a polishing cloth (Mark V Laboratory, East Granby, CT). The gold electrode was polished with fine grade emery papers. Both glassy carbon and gold electrodes rinsed in deionized water.

Potential sweep rate was 10 mVs^{-1} in cyclic voltammetry. Both cyclic voltammetry and chronoamperometry studies were carried out at room temperature and in unstirred solutions.

The examination of the crystal structure of the films was carried out on Siemens D 5000 (computer controlled) powder diffractometer with an iron filter Co-Kα radiation for the electrodeposition alloy films on stainless steel substrate of composition 5:5 of (0.1 M $CdSO_4$:0.1 M SeO_2) in 1 M sulfuric acid bath. Optical measurement of samples deposited on stainless steel substrate was carried out using a Jasco, UV-Visible-NIR spectrophotometer within the wavelength range of 190–500 nm. Electroconductivity measurements were carried out in the frequency range 100 Hz by using an LCR meter type AG-411B (Ando electric Ltd. Japan).

3 Results and discussion

3.1 Cyclic voltammetry

Cyclic voltammetry was used to monitor the electrochemical reactions in solutions 0.1 M $CdSO_4$, 0.1 M SeO_2 and mixtures, in order to find the suitable CdSe deposition potential range. The deposition potential of CdSe alloy shifted to more negative value than the deposition potential of the individual metals, as the concentration of Se^{2-} ions increases in the mixture, as shown in Figs. 1 and 2.

Also, inspecting the cyclic voltammograms for the electrodeposition of CdSe alloy on glassy carbon electrode

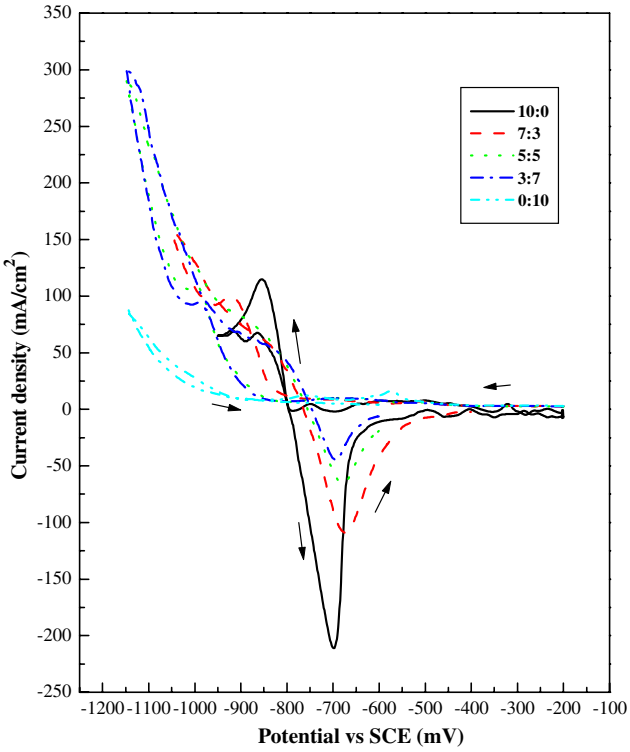

Fig. 1 Cyclic voltammogram for the electrodeposition of CdSe alloy on glassy carbon electrode from 0.1 M $CdSO_4$:0.1 M SeO_2 solutions of various ratios in 1 M sulfuric acid at scan rate 10 mV s^{-1} and at room temperature

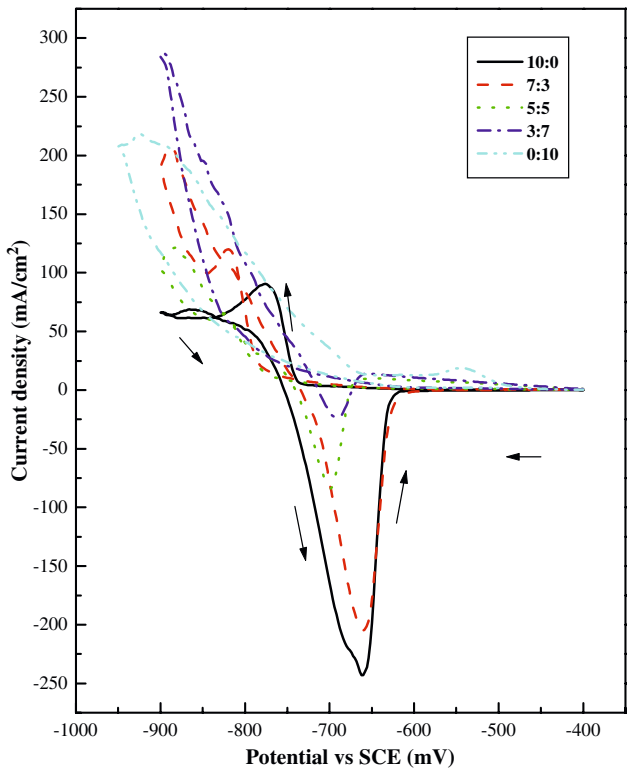

Fig. 2 Cyclic voltammogram for the electrodeposition of CdSe alloy on gold electrode from 0.1 M $CdSO_4$:0.1 M SeO_2 solutions of various ratios in 1M sulfuric acid at scan rate 10 mV s^{-1} and at room temperature

from various ratios of Cd^{2+}:Se^{4+} in 1 M H_2SO_4 solution at ''v'' = 10 mV s^{-1} and at room temperature, increasing the Se^{4+} concentration in the bath from 10:0 to 7:3 shifts the deposition potential to more negative value while the oxidation potential peak shifts to more positive value, further increasing of Se^{4+} content in the solution the reduction potential exhibits an intermediate value between zero Se^{4+} and Cd^{2+}:Se^{4+} (7:3) ratio on the electrode surface.

On the surface of gold electrode, the same reduction behaviour is obtained, while for the anodic scan, the increase in Se^{4+} content shifts the oxidation potential to less positive value.

Table 1 The ratio of the cathodic to anodic charge obtained for deposition of cadmium selenide on different electrodes

Bath Composition 0.1 M (equimolar)	Ratio of the charge	
	Glassy carbon electrode	Gold electrode
10:0	0.61	0.82
7:3	0.08	0.69
5:5	0.18	0.89
3:7	0.10	0.27
0:10	0.16	0.47

Mechanism of CdSe electrodeposition onto the two substrates either glassy carbon or gold surface took place simultaneously at potentials –872 and –778.8 mV, respectively. Where Cd^{2+} is reduced to Cd on the surface of the substrate [20], hence simultaneously CdSe alloy is formed by underpotential deposition (UPD) mechanism.

$$Cd^{2+} + 2e^- \leftrightarrow Cd \quad (1)$$

$$SeO_2 + H_2O \leftrightarrow H_2SeO_3 \quad (2)$$

$$Cd + H_2SeO_3 + 4H^+ + 4e^- \leftrightarrow CdSe + 3H_2O \quad (3)$$

According to Natarajan et al. [21] the excess deposited selenium with the single phase CdSe alloy may be attributed to the following reactions:

$$Se + 2H^+ + 2e^- \leftrightarrow H_2Se \quad (4)$$

$$2H_2Se + H_2SeO_3 \leftrightarrow 3Se + 3H_2O \quad (5)$$

reaction (6) being the source of the excess selenium.

Table 1 shows the ratio of the cathodic to anodic charge, with respect to concentration. The results indicate that a large amount of hydrogen evolved in competition with the

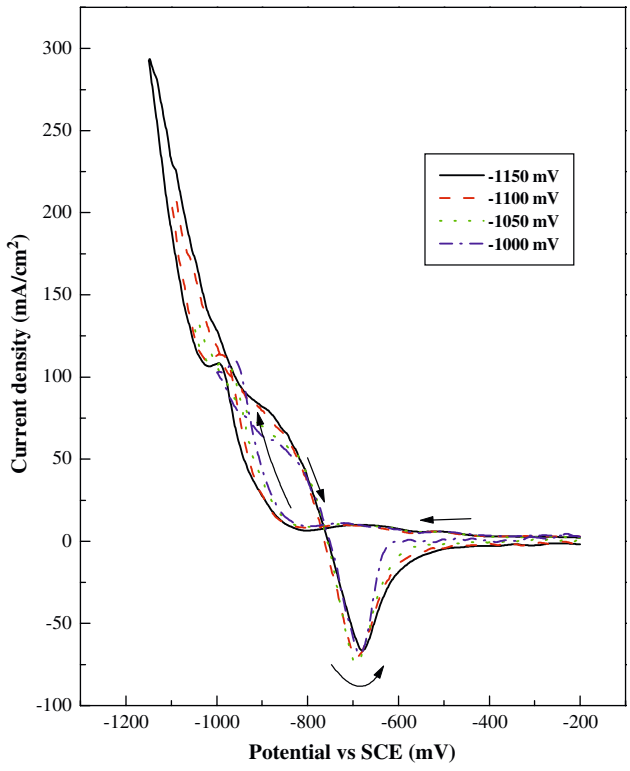

Fig. 3 Cyclic voltammetry for the effect of decreasing cathodic scan limit at glassy carbon electrode in 5:5 (0.1 M $CdSO_4$:0.1 M SeO_2) in 1 M sulfuric acid, scan rate 10 mV s^{-1} and at room temperature

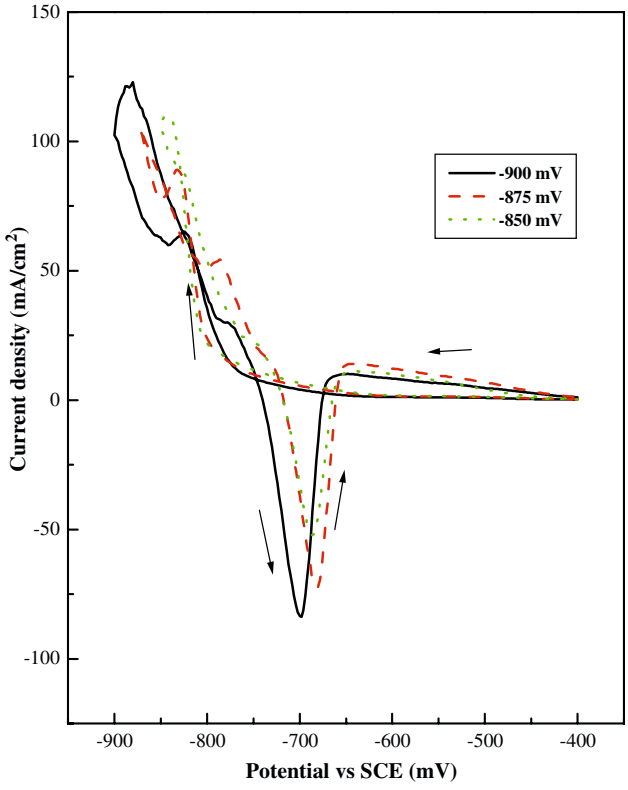

Fig. 4 Cyclic voltammetry for the effect of decreasing cathodic scan limit at gold electrode in 5:5 (0.1 M $CdSO_4$:0.1 M SeO_2) in 1 M sulfuric acid, scan rate 10 mV s^{-1} and at room temperature

deposition process, on glassy carbon electrode. Meanwhile, on gold electrode the major electrode reaction is the cadmium selenide alloy deposition. This may be attributed to the difference in nature between glassy carbon and gold electrodes.

The effect of decreasing cathodic scan limit on the cyclic voltammograms of the two electrodes, is shown in Figs. 3 and 4. As the cathodic scan limit shifts in the less negative direction, the deposition potential of CdSe shifts to less negative value with glassy carbon electrode, but with gold electrode the deposition potential of CdSe shifts to more negative value. It is seen that a noticeable CdSe deposition starts at about –872 mV with glassy carbon electrode and at –778.8 mV with gold electrode. This means that the deposition of CdSe alloy is more easier on gold electrode than glassy carbon electrode.

Figure 5 displays the relation between peak potential ''E_p'' for the alloy vs. log υ and peak current density $I_{p,c}$ vs. $v^{1/2}$, whereas ''v'' increases ''E_p'', values are shifted to more negative values and ''I_p'' values are increased. The linear dependence of E_p vs. log v and I_p vs. $v^{1/2}$ indicate that the reduction process is under diffusion control.

Elevating the bath temperature decreases the alloy deposition potential, Fig. 6. This behaviour may be attributed to the depolarization effect of temperature on the discharge overpotential of the reducible ions (Cd^{2+}, Se^{2+} and H^+). Also, the increase in temperature enhances hydrogen discharge processes.

From Fig. 7 the activation energy of the diffusional process can be calculated as Ea = 9.7 kJ mol^{-1} for deposition on glassy carbon electrode and Ea = 50.4 kJ mol^{-1} for deposition on gold electrode.

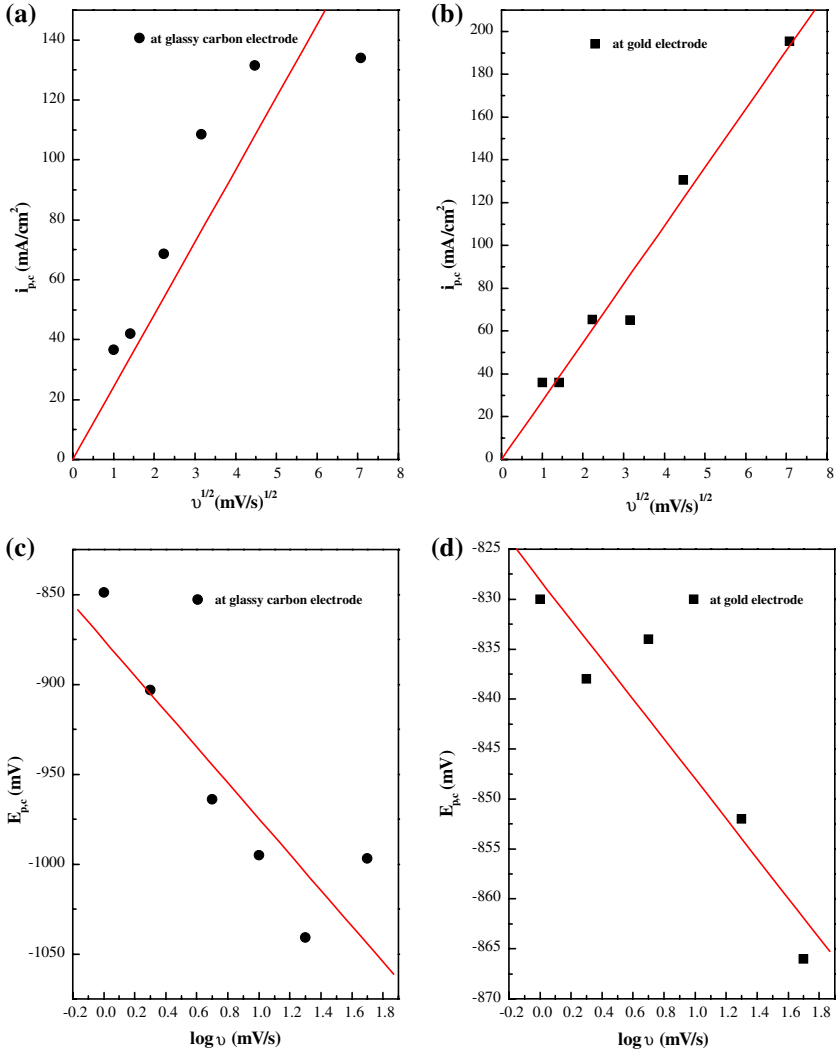

Fig. 5 (**a**,**b**) peak current density $i_{p,c}$ and (**c**,**d**) peak potential $E_{p,c}$ vs. scan rate v for cyclic voltammograms recorded in acidic 5:5 (0.1 M $CdSO_4$:0.1 M SeO_2) solution

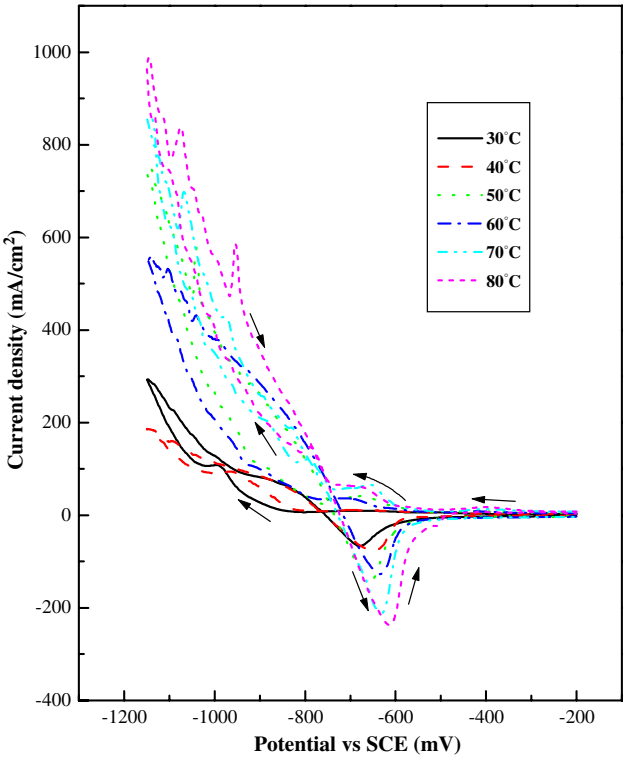

Fig. 6 Cyclic voltammetry for the effect of temperature at glassy carbon electrode in 5:5 (0.1 M $CdSO_4$:0.1 M SeO_2) in 1 M sulfuric acid at scan rate 10 mV s^{-1}

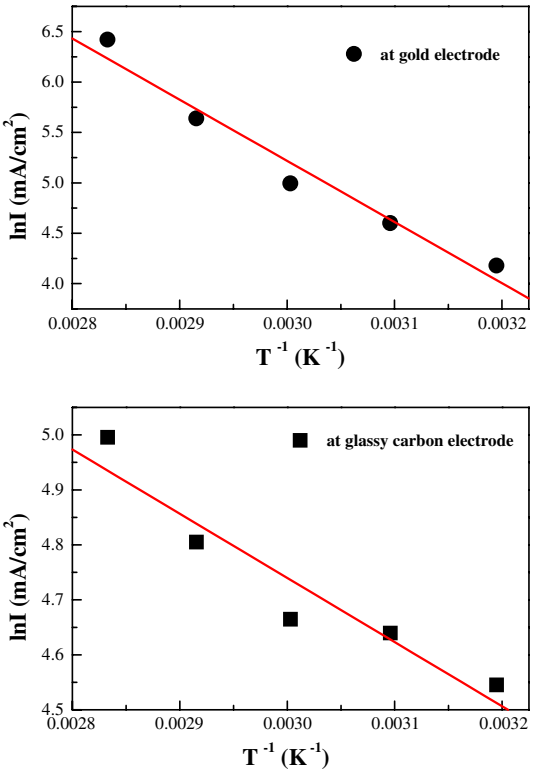

Fig. 7 Arrhenius plot for cadmium selenid reduction, from 5:5 (0.1 M $CdSO_4$:0.1 M SeO_2) in 1 M sulfuric acid solution

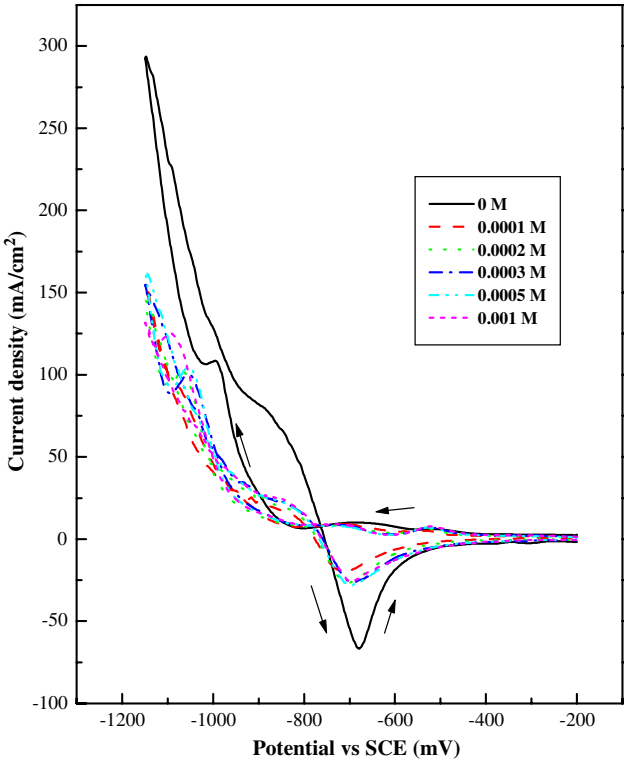

Fig. 8 Cyclic voltammetry for the effect of addition of SDS at glassy carbon electrode to 5:5 (0.1 M $CdSO_4$:0.1 M SeO_2) in 1 M sulfuric acid at scan rate 10 mV s^{-1} and at room temperature

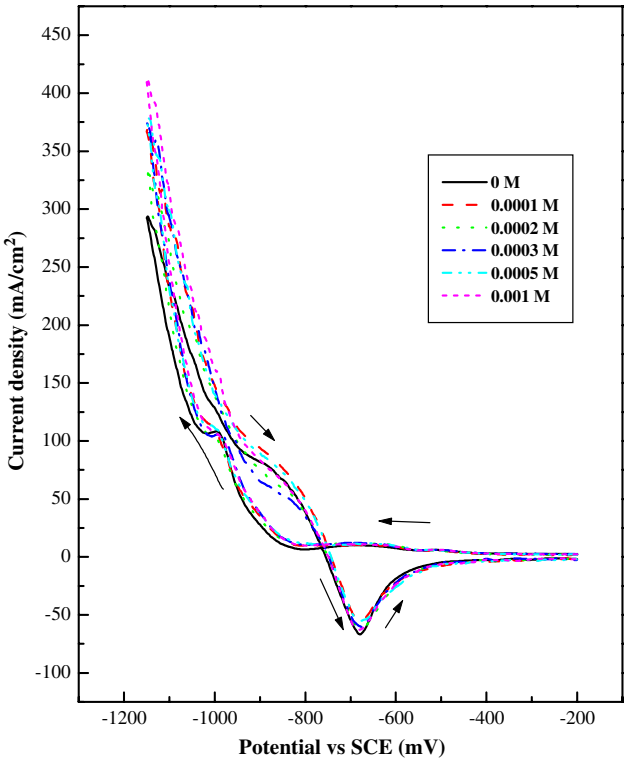

Fig. 9 Cyclic voltammetry for the effect of addition of sodium gluconate at glassy carbon electrode to 5:5 (0.1 M $CdSO_4$:0.1 M SeO_2) in 1 M sulfuric acid at scan rate 10 mV s^{-1} and at room temperature

Table 2 Surface coverage values (Γ) obtained for different concentrations of SDS and sodium gluconate

Γ (atom·cm^{-2})	SDS		Sodium gluconate	
$C_{additive}$(mole·L^{-1})	Glassy carbon electrode	Gold electrode	Glassy carbon electrode	Gold electrode
1×10^{-4}	3.16×10^{18}	1.11×10^{18}	6.56×10^{18}	1.94×10^{18}
2×10^{-4}	3.07×10^{18}	1.1×10^{18}	6.16×10^{18}	1.68×10^{18}
3×10^{-4}	3.37×10^{18}	9.23×10^{17}	6.79×10^{18}	2.28×10^{18}
5×10^{-4}	3.35×10^{18}	7.39×10^{17}	6.73×10^{18}	2.73×10^{18}
1×10^{-3}	3.45×10^{18}	1.21×10^{18}	7.06×10^{18}	2.4×10^{18}

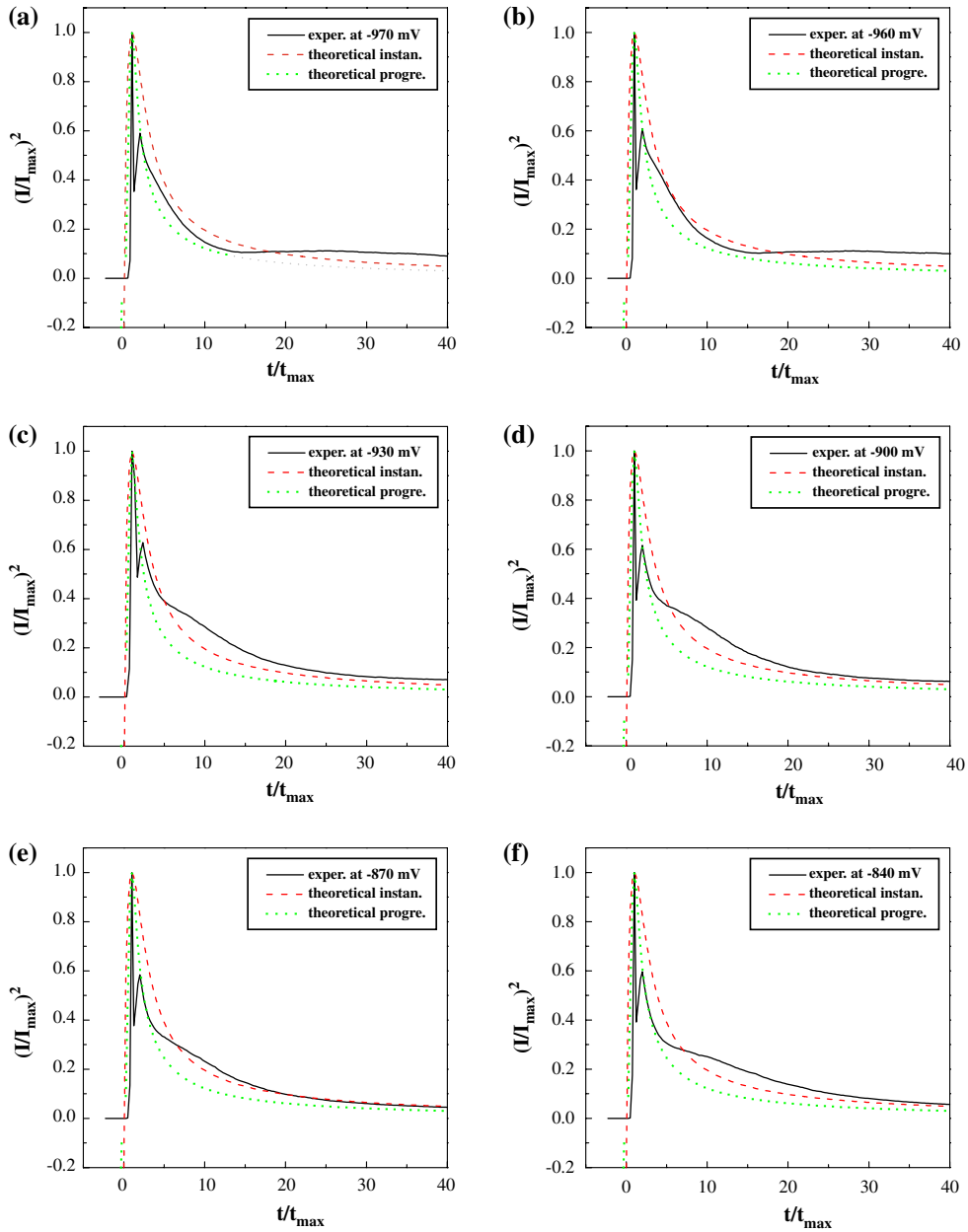

Fig. 10 Comparison between experimental points for cadmium selenide deposition on glassy carbon electrode,and the theoretical nondimensional plots for instantaneous and progressive nucleation models

The effect of adding sodium dodecyl sulfate, is shown in Fig. 8. It shows that the addition of SDS shifts the deposition potential of CdSe alloy to more negative value as the concentration of SDS increases and the ''$I_{p,c}$'' decreases than additive free solution. This means that the deposition of CdSe is retarded as the concentration of SDS increases. The same behaviour is noticed with using gold electrode.

Figure 9 shows the effect of adding sodium gluconate on cyclic voltammograms at the two electrodes. It reveals that the deposition potential of cadmium selenide alloy is shifted slightly to less negative value with increasing the concentration of sodium gluconate, while ''$I_{p,c}$'' has no change. Also, with using gold electrode, the same behaviour is recorded with higher ''$I_{p,c}$'' than additive free solution.

The surface coverage for both additives on different substrates, is shown in Table 2. The results reveal that as the concentration of additive increases the surface coverage ''Γ'' is promoted, except in case of SDS with gold electrode. Also, the highest ''Γ'' noticed for 1×10^{-3} M additive, expect in case of sodium gluconate with gold electrode.

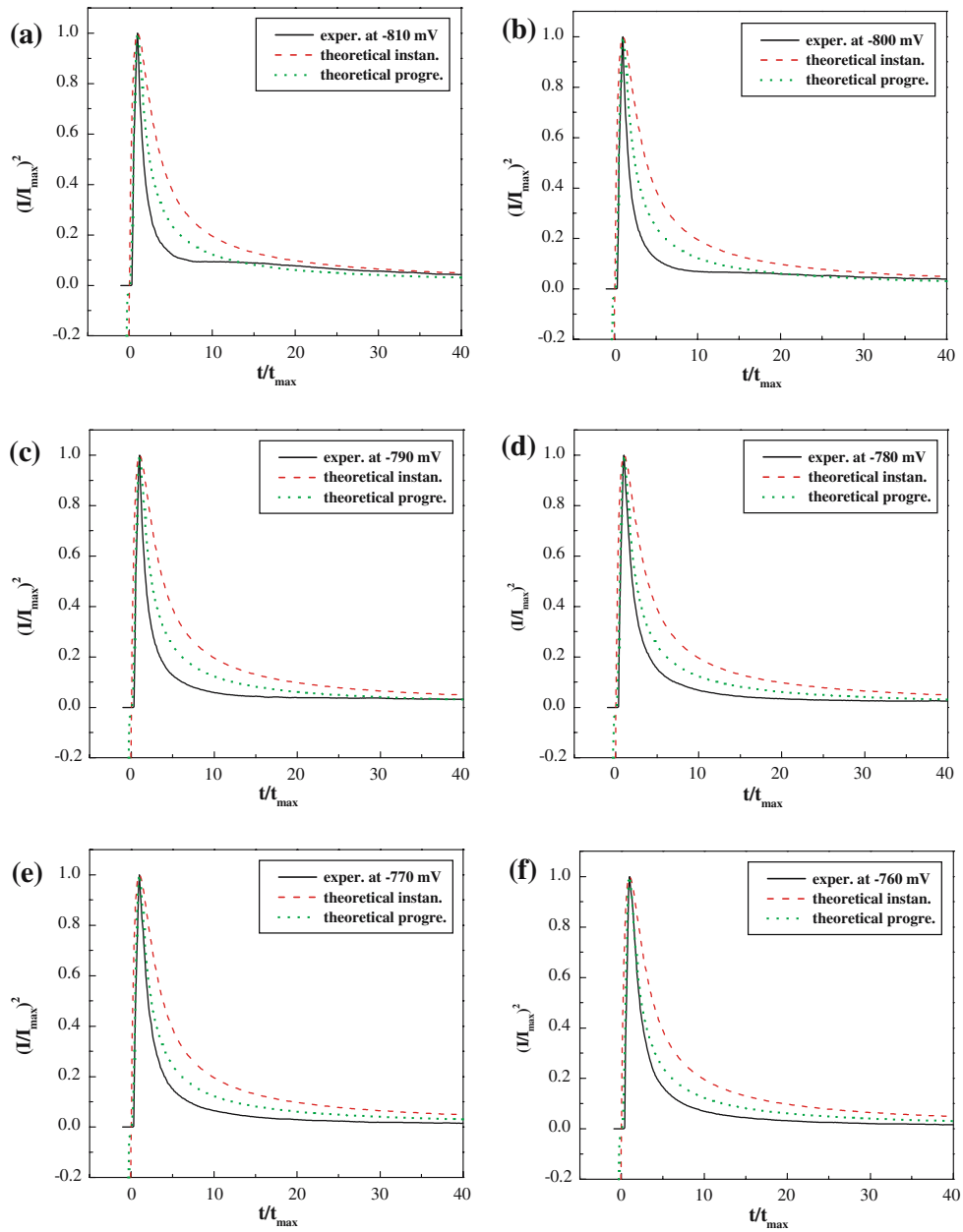

Fig. 11 Comparison between experimental points for cadmium selenide deposition on gold electrode, and the theoretical nondimensional plots for instantaneous and progressive nucleation models

3.2 Chronoamperometry

Figures 10 and 11 display the comparison between experimental points for CdSe deposition on the two cathodes, and the theoretical nondimensional plots for instantaneous and progressive nucleation models. It is clear that the results follow closely to the progressive nucleation model at all applied potentials. So, the electrodeposition of CdSe from the acidic solution of ratio 5:5 from (0.1 M cadmium sulfate:0.1 M selenium dioxide) follows the mechanism of progressive nucleation and growth, at the two electrodes surfaces.

Figures 12 and 13 show the theoretical and nondimensional plots for the experimental effect of temperature on current-time curves for the deposition of cadmium selenide on glassy carbon and gold electrodes, respectively. The results indicate that the mechanism of CdSe film deposition follows the mechanism of progressive nucleation and growth, at all studied temperatures.

Table 3, illustrates the saturated nucleation density, N_{sat}, and the nucleation rate constant, A. It is clear from the data that the temperature has no effect on N_{sat} at glassy carbon electrode, while at gold electrode it has a little effect.

3.3 Structure of the deposits

Figure 14(i) shows the X-ray diffraction pattern of the deposited films of crystalline CdSe alloy on the stainless steel substrate. At low current density, the alloy is crystallized in the form of hexagonal shape with two different planes (110) and (201). Upon increasing the current density to 2.5 A dm^{-2} as depicted in Table 4, the alloy is deposited

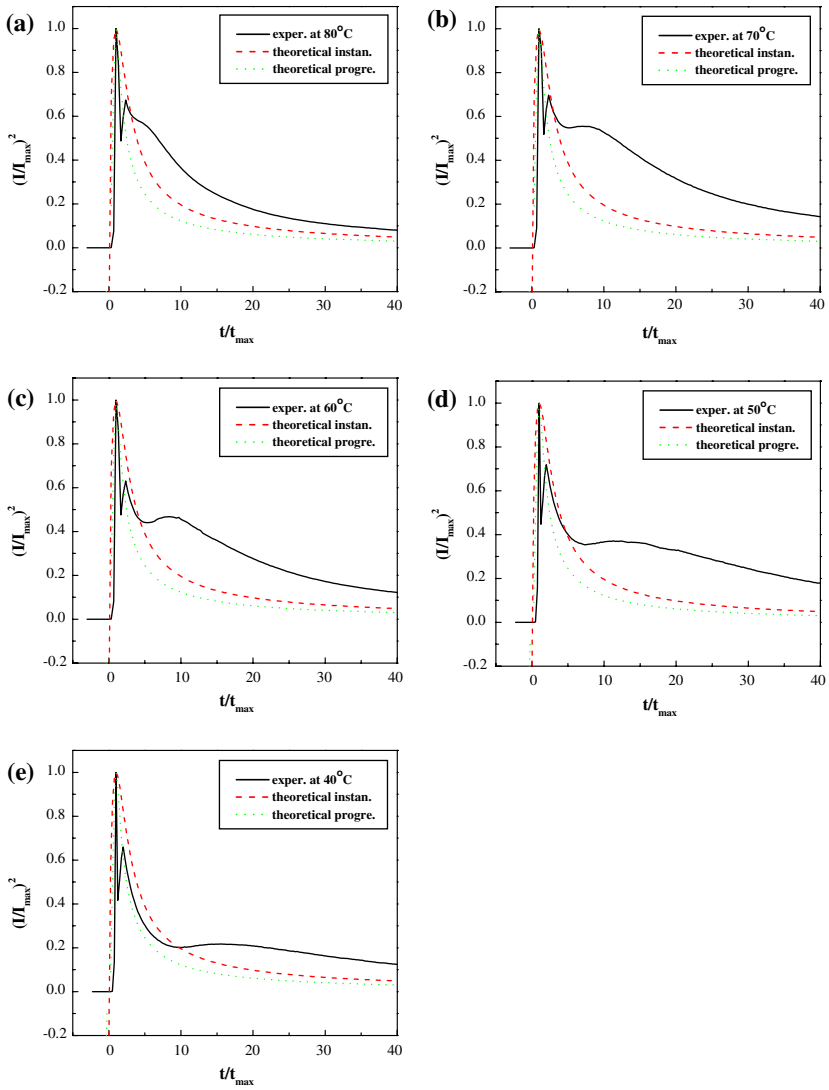

Fig. 12 Comparison between experimental points for cadmium selenide deposition on glassy carbon electrode,and the theoretical nondimensional plots for instantaneous and progressive nucleation models for curves in Fig. 15a

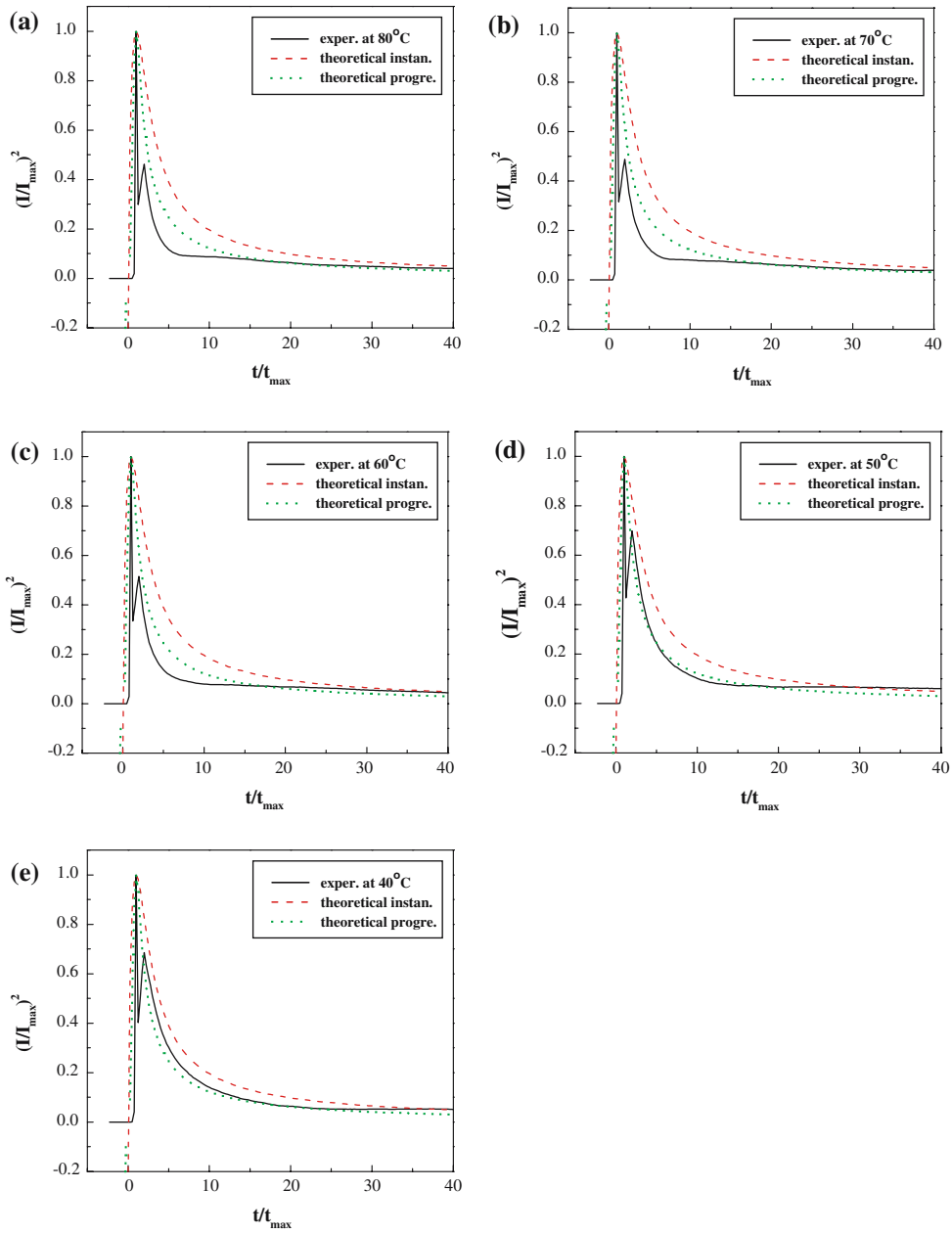

Fig. 13 Comparison between experimental points for cadmium selenide deposition on gold electrode,and the theoretical nondimensional plots for instantaneous and progressive nucleation models for curves in Fig. 15b

Table 3 Saturated nucleation density, N_{sat}, and the nucleation rate constant, A, values for electrodeposition of cadmium selenide from composition 5:5 of (0.1 M $CdSO_4$:0.1 M SeO_2) in 1 M sulfuric acid bath, on solid electrodes surfaces and under different temperatures

Temperature (°C)	Glassy carbon electrode		Gold electrode	
	$N_{sat}(cm^{-2})$	A ($cm^{-2}s^{-1}$)	$N_{sat}(cm^{-2})$	A($cm^{-2}s^{-1}$)
40	4.97×10^{15}	8.57×10^{17}	1.88×10^{15}	3.27×10^{17}
50	5.73×10^{15}	9.88×10^{17}	1.89×10^{15}	3.26×10^{17}
60	5.31×10^{15}	1.22×10^{18}	1.36×10^{15}	2.34×10^{17}
70	5.91×10^{15}	1.36×10^{18}	1.13×10^{15}	1.95×10^{17}
80	4.98×10^{15}	1.14×10^{18}	8.66×10^{14}	1.49×10^{17}

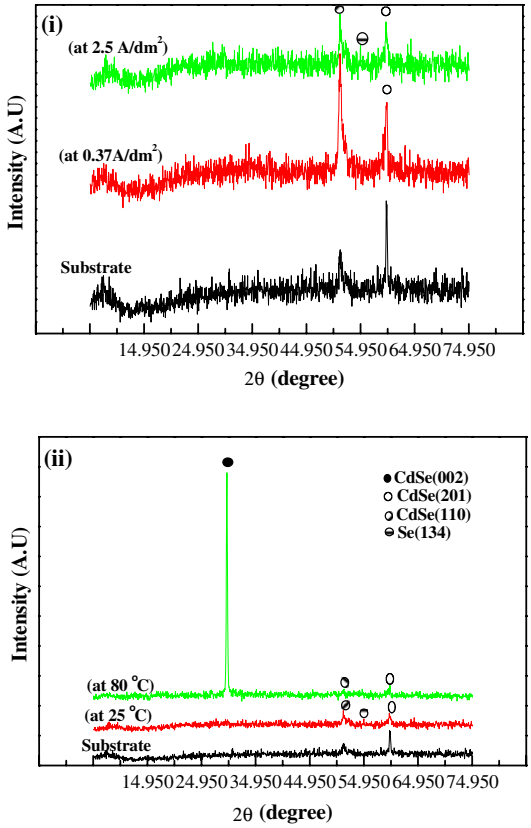

Fig. 14 X-ray diffraction patterns of electrodeposited cadmium selenide alloy from a bath containing 0.1 M $CdSO_4$ and 0.1 M SeO_2 in 1 M sulfuric acid solution and deposition time = 30 min. (**i**) At different current densities, (**ii**) at different temperatures

in its hexagonal form in addition to the deposition of single selenium metal in monoclinic form with a characteristic plane (134) [22].

The effect of temperature on the microcrystalline form of the deposits is shown in Fig. 14(ii). Upon increasing temperature of the electrolytic bath solution from 25 to 80 °C, the alloy is deposited in its hexagonal form with

Table 4 X-ray diffraction data for the as-electrodeposited cadmium selenide alloy obtained from a bath containing solution of ratio 5:5 from (0.1 M cadmium sulfate:0.1 M selenium dioxide) in 1 M sulfuric acid, deposition time = 30 min., room temperature and at different current densities

Current density (A/dm^2)	2θ(degree)	d(A°)	hkl	phase	structure
[a]0.37	51.20	2.071	(110)	CdSe	Hexagonal
	59.7	1.795	(201)	CdSe	Hexagonal
[b]2.5	51.35	2.070	(110)	CdSe	Hexagonal
	52.15	2.035	(134)	Se	Monoclinic
	59.65	1.797	(201)	CdSe	Hexagonal

[a] at deposition potential = –535 mV

[b] at potential = –725 mV

Table 5 X-ray diffraction data for the as-electrodeposited cadmium selenide obtained from a bath containing solution of ratio 5:5 from (0.1 M cadmium sulfate:0.1 M selenium dioxide) in 1 M sulfuric acid at potential = –725mV, deposition time = 30 min., and at different temperatures

Temperature(°C)	2θ(degree)	d(A°)	hk1	phase	structure
25	51.35	2.070	(110)	CdSe	Hexagonal
	52.15	2.035	(134)	Se	Monoclinic
	59.65	1.797	(201)	CdSe	Hexagonal
80	29.65	3.498	(002)	CdSe	Hexagonal
	51.3	2.070	(110)	CdSe	Hexagonal
	59.7	1.795	(201)	CdSe	Hexagonal

decreasing of the intensity of the two characteristic planes for CdSe alloy (110) and (201). A new plane is observed (002) which could be assigned also for CdSe alloy as in Table 5. The deposition of free selenium did not occur at high temperature.

3.4 Optical absorption studies

The linear correlation analysis of the experimental data from the linear trend of the $(\alpha\ h\nu)^n$ versus $(h\upsilon)$ dependence, indicates $n = 2$, hence cadmium selenide is a direct type of semiconductors, as shown in Fig. 15. The spectral region is the region of intrinsic absorption of deposited films and the electronic transitions are of direct allowed type (band to band transitions). The calculated band gap energy is 3.56 eV. The obtained value is higher than that of bulk alloy. Such differences may attributed to preparative methods. The magnitude of absorption coefficient is of the

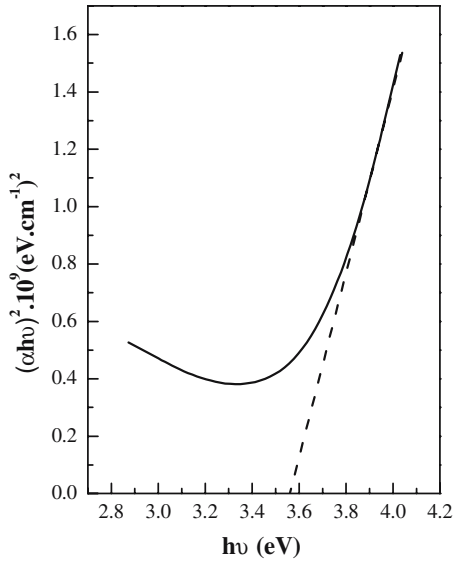

Fig. 15 The $(\alpha\ h\nu)^2$ vs $h\nu$ dependence for CdSe deposited at room temperature, on stainless steel substrates

Table 6 Specific resistivety (R), resistance (ρ), electrical conductivity (δ), the concentration of charge carriers (n), and mobility of the charge carriers (μ) values at deposition potential = –535 mV, for cadmium selenide alloy deposition from solution of volumetric proportion 5:5 from (0.1 M cadmium sulfate:0.1 M selenium dioxide) in 1 M sulfuric acid bath on stainless steel substrate

Frequency (Hz)	R (Ω)	ρ (Ω cm^{-1})	δ (Ω^{-1} cm)	n	μ (cm^2 V^{-1} s^{-1})
0.1	5,160	0.53786	1.85922	1.4×10^{46}	8.51069E-28
0.2	5,070	0.528479	1.892224	1.4×10^{46}	8.66176E-28
0.3	4,800	0.500335	1.998662	1.4×10^{46}	9.14899E-28
0.5	4,746	0.494706	2.021403	1.4×10^{46}	9.25309E-28
1	4,710	0.490953	2.036853	1.4×10^{46}	9.32381E-28
2	4,673	0.487097	2.05298	1.4×10^{46}	9.39763E-28
5	4,650	0.484699	2.063135	1.4×10^{46}	9.44412E-28
10	4,641	0.483761	2.067136	1.4×10^{46}	9.46243E-28
25	4,652	0.484908	2.062248	1.4×10^{46}	9.44006E-28
50	4,670	0.486784	2.054299	1.4×10^{46}	9.40367E-28
100	4,690	0.488869	2.045539	1.4×10^{46}	9.36357E-28

order of 10^4 cm^{-1} which is in agreement with the range of semiconductors [23].

3.5 Electrical conductivity

The measured electrical conductivity value for cadmium selenide alloy was found to be in the range of semiconductor materials [24], as shown in Table 6. The mobility of the charge carriers for CdSe is small according to high concentration of charge carriers.

4 Conclusions

The CdSe films, prepared by electrodeposition technique, have hexagonal structure. The optical band gap is found to be 3.56 eV. Electrical resistivity of CdSe film is of the order of 10^4 Ω.

References

1. A.K. Pal, A. Mondal, S. Chaudhuri, Vacuum **41**, 1460 (1990)
2. T. Cruszecki, B. Holmstrom, Sol. Energy Mater. Sol. Cells **31**, 227 (1993)
3. S. Ericsson, T. Cruszecki, P. Carlsson, B. Holmström, Thin Solid Films **269**, 14 (1995)
4. A. van Calster, F. Vanfleteren, I. de Rycke, J. de Baets, J. Appl. Phys. **64**, 3282 (1988)
5. N.G. Patel, C.J. Panchal, K.K. Makhijia, Cryst. Res. Technol. **29**, 1013 (1994)
6. V.A. Smyntyana, V. Gerasutenko, S. Kashulis, G. Mattogno, S. Reghini, Sensors Actuators **19**, 464 (1994)
7. B. Bonello, B. Fernandez, J. Phys. Chem. Solids **54**, 209 (1993)
8. J.C. Schottmiller, R.W. Francis, C. Wood, US patent, 3884688, (1975)
9. B.J. Curtis, H. Kiess, H.R. Brunner, K. Frick, Photogr. Sci. Eng. **24**, 244 (1980)
10. G.M. Fofanov, G.A. Kitaev, Russ. J. Inorg. Chem. **14**, 322 (1969)
11. O. Portillo-Moreno, R. Lozda-Morales, M. Rubin Falfán, J.A. Pérez-Álvarez, O. Zelaya-Angel, L. Baños-Lórez, J. Phys. Chem. Solids **61**, 1751(2000)
12. R. Lozda-Morales, et al. J. Electrchem. Soc. **146**, 2546 (1999)
13. S. Gorrer, G. Hodes, Phys. Rev. **36**, 4215 (1987)
14. R.C. Kainthla, D.K. Pandya, K.L. Chopra, J. Electrochem. Soc. **127**, 277 (1980)
15. R.C. Kainthla, D.K. Pandya, K.L. Chopra, J. Electrochem. Soc. **129**, 99 (1980)
16. N. Samarth, H. Luo, J.K. Furdyone, S.B. Quadvi, Y.R Lee, A.K. Ramdas, N. Otsuka, Appl. Phys. Lett. **54**, 2162 (1989)
17. L.P. Colletti, B.H. Flowers, J.L. Stickney, J. Electrochem. Soc. **145**, 1442 (1998)
18. T. Hayashi, R. Saeki, T. Suzuki, M. Fukaya, Y. Ema, J. Appl. Phys. **38**, 5719 (1990)
19. B. Pejova, A. Tanuševski, I. Grozdanov, J. Solid State Chem. **172**, 381 (2003)
20. Cheng-min Shen, Xiao-gang Zhang, Hu-lin Li, J. Mater. Sc. and Engineering, B **84**, 265 (2001)
21. C. Natarajan, M. Sharon, C.Lévy-CLément, M. Neumann-Spallar, Thin Solid Films **237**, 118 (1994)
22. NBS Circular, 539, 7, 12(1957)
23. R.B. Kale, S.D. Sartale, B.K. Chougule, C.D. Lokhande, J. Semicond. Sci. Technol. **19**, 980 (2004)
24. R.B. Kale, C.D. Lokhande, J. Semicond. Sci. Technol. **20**, 1 (2005)